

Understanding top-of-atmosphere flux bias in the AeroCom Phase III models: a clear-sky perspective

Wenying Su¹, Lusheng Liang², Gunnar Myhre³, Tyler J Thorsen¹, Norman G. Loeb¹, Gregory L. Schuster¹, Paul Ginoux⁴, Fabien Paulot⁵, David Neubauer⁶, Ramiro Checa-Garcia⁷, Hitoshi Matsui⁸, Kostas Tsigaridis⁹, Ragnhild Bieltvedt Skeie¹⁰, Toshihiko Takemura¹¹, Susanne E. Bauer¹², and Michael Schulz¹³

¹NASA Langley Research Center

²Science Systems & Applications Inc.

³CICERO, Norway

⁴NOAA GFDL

⁵NOAA/GFDL

⁶ETH Zurich

⁷Laboratoire des Sciences du Climat et de l'Environnement, IPSL

⁸Nagoya University

⁹Center for Climate Systems Research, Columbia University, and NASA Goddard Institute for Space Studies

¹⁰Center for International Climate and Environmental Research - Oslo (CICERO)

¹¹Kyushu University

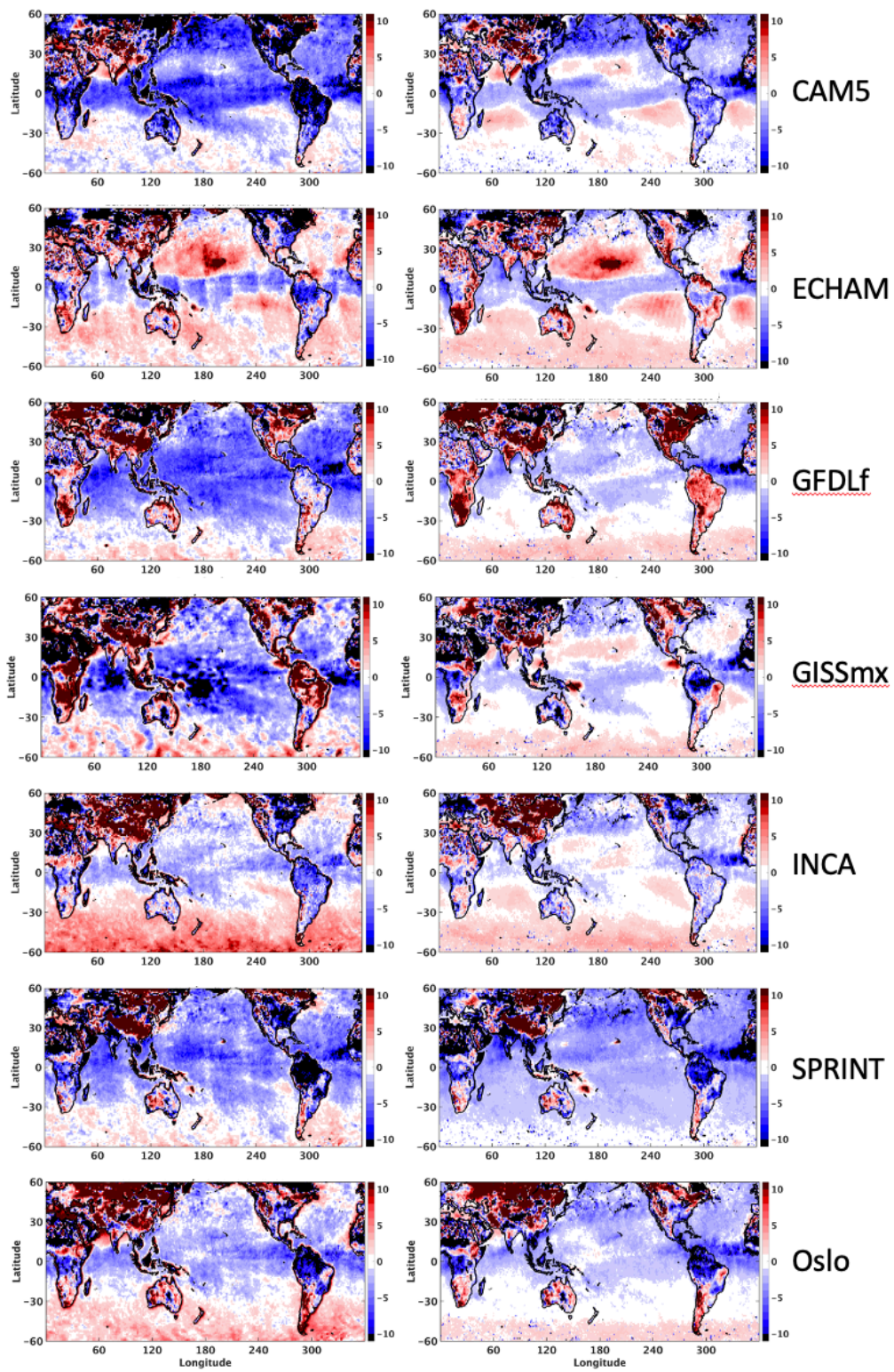
¹²NASA Goddard Institute for Space Studies, New York, NY, USA

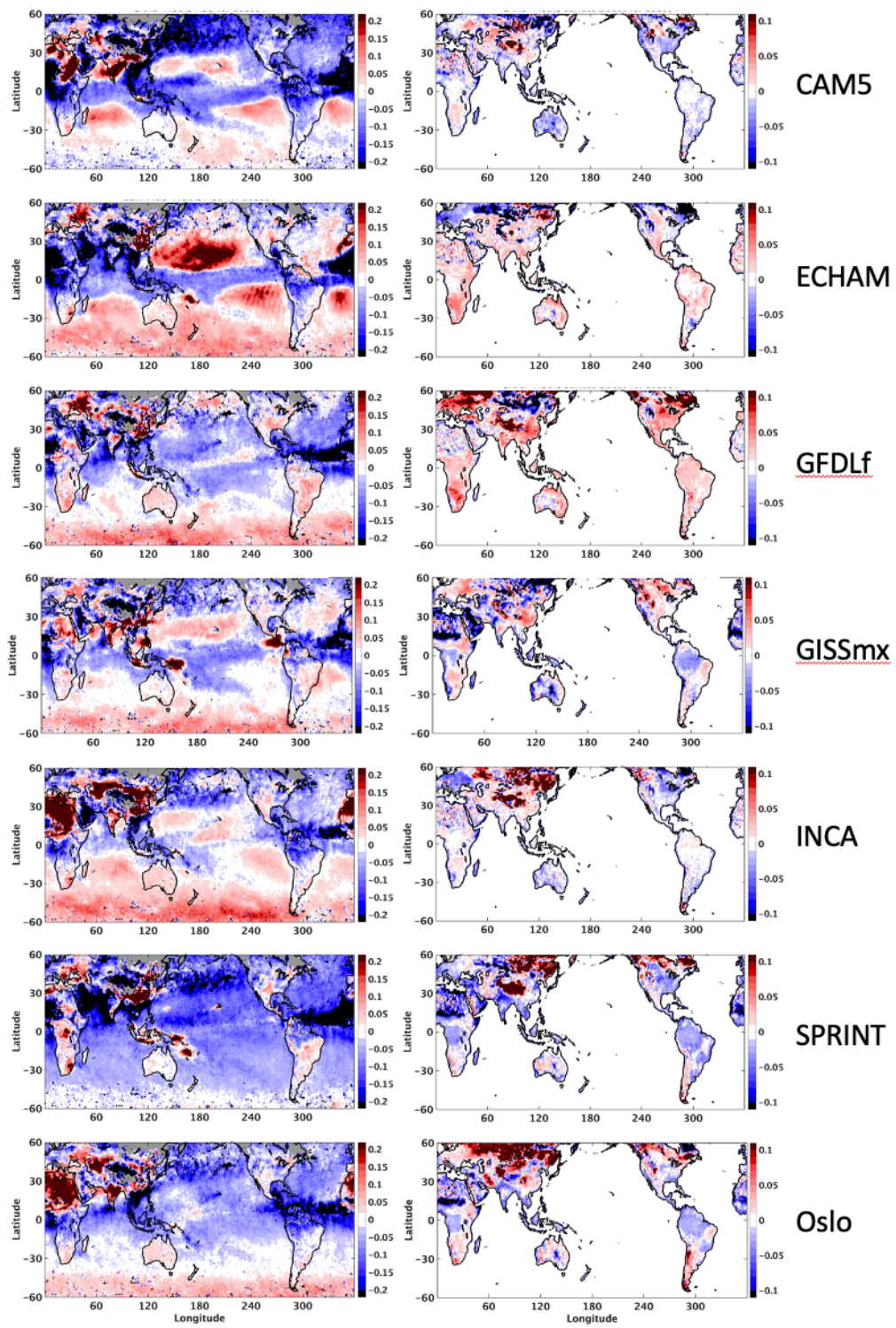
¹³Norwegian Meteorological Institute

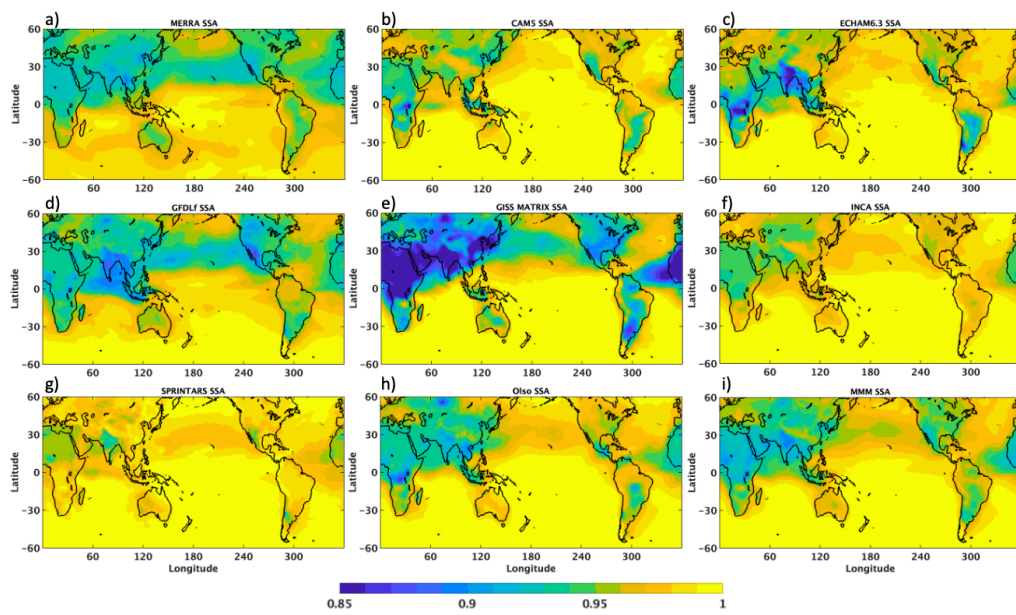
November 22, 2022

Abstract

Biases in aerosol optical depths (AOD) and land surface albedos in the AeroCom models are manifested in the top-of-atmosphere (TOA) clear-sky reflected shortwave (SW) fluxes. Biases in the SW fluxes from AeroCom models are quantitatively related to biases in AOD and land surface albedo by using their radiative kernels. Over ocean, AOD contributes about 25% to the 60°S-60°N mean SW flux bias for the multi-model mean (MMM) result. Over land, AOD and land surface albedo contribute about 40% and 30%, respectively, to the 60°S-60°N mean SW flux bias for the MMM result. Furthermore, the spatial patterns of the SW flux biases derived from the radiative kernels are very similar to those between models and CERES observation, with the correlation coefficient of 0.6 over ocean and 0.76 over land for MMM using data of 2010. Satellite data used in this evaluation are derived independently from each other, consistencies in their bias patterns when compared with model simulations suggest that these patterns are robust. This highlights the importance of evaluating related variables in a synergistic manner to provide an unambiguous assessment of the models, as results from single parameter assessments are often confounded by measurement uncertainty. We also compare the AOD trend from three models with the observation-based counterpart. These models reproduce all notable trends in AOD (i.e. decreasing trend over eastern United States and increasing trend over India) except the decreasing trend over eastern China and the adjacent oceanic regions due to limitations in the emission dataset.







F

http://doi.org/10.1029/2019MS001710
Manuscript accepted: 18 September 2020
Editorial handling: Michael W. Hines

Manuscript ID: 2019MS001710
Version: 1

Submitted: 10 August 2019

Revised: 10 January 2020

Accepted: 10 February 2020

Published online: 10 March 2020

Manuscript first published online: 10 March 2020

Editorial handling: Michael W. Hines

Manuscript ID: 2019MS001710
Version: 1

Submitted: 10 August 2019

Revised: 10 January 2020

Accepted: 10 February 2020

Published online: 10 March 2020

Editorial handling: Michael W. Hines

Manuscript ID: 2019MS001710
Version: 1

Submitted: 10 August 2019

Revised: 10 January 2020

Accepted: 10 February 2020

Published online: 10 March 2020

Editorial handling: Michael W. Hines

Manuscript ID: 2019MS001710
Version: 1

Submitted: 10 August 2019

Revised: 10 January 2020

Accepted: 10 February 2020

Published online: 10 March 2020

Editorial handling: Michael W. Hines

Manuscript ID: 2019MS001710
Version: 1

Submitted: 10 August 2019

Revised: 10 January 2020

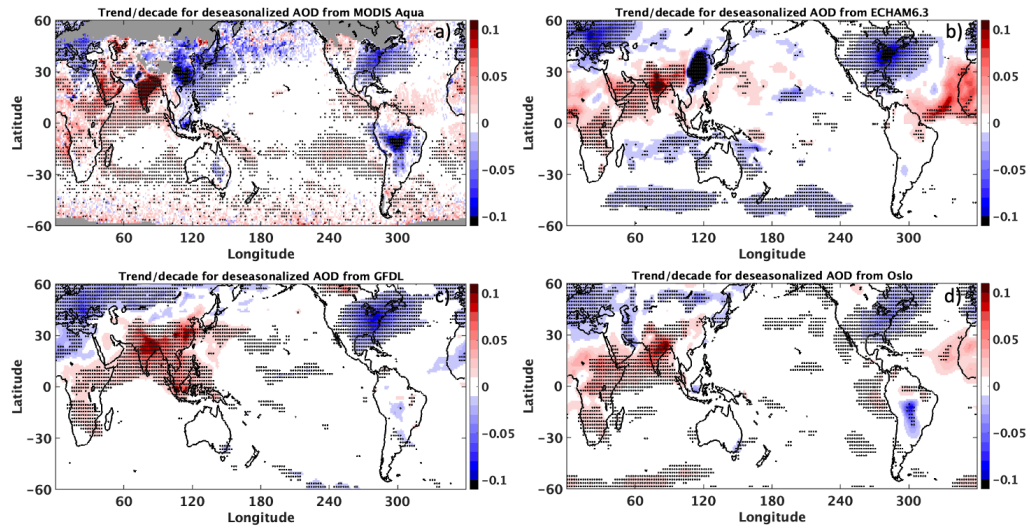
Accepted: 10 February 2020

Published online: 10 March 2020

Editorial handling: Michael W. Hines

F.

F.



F

golfball
hockey
hockey
hockey
hockey
hockey
hockey
hockey
hockey
hockey

THE SHOW
ffair
le
le 2021)

DARE F(; ff;)X- F(AOD; ff;)X 3)

bv ff ishish
~~emph~~

X

DARE $\vdash (\lambda x. x) \circ (\lambda y. y)$ (AOD; 4)

Why the hell
isn't it possi-
ble to fill

FDARE ~~and~~

$$\text{fDARE} = \text{fF}(ff) - \text{fF}(AOD; ff;)X \quad (5)$$

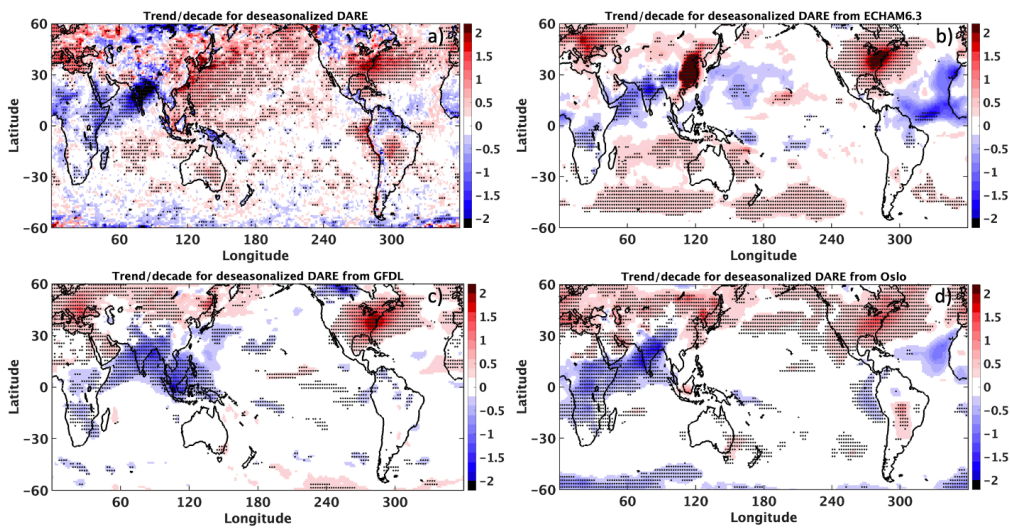
fff (AOD; ff;)~~K~~

E 2 SW

10

Philip H. Phillips
Editor-in-Chief
Volume 16
Law & Order
Principles &
Problems

Diffusion

*F*

2

2

	E 2540	N 10120)	T 22	N 090)	S 042	N 65283)
B	04	03		19	03		12	03	
M	18	08		07	03		16	03	
D	00	03		08	02		13	02	
S	02	02		11	03		10	02	

Figure 13.

$$A \qquad A$$

ABAB is ~~the~~ **the**

A D

THE END

A

ESTATE PLANNING

- Digitized by**
University of
Illinois
Urbana-Champaign
Digitized by

1994) **A**
B
C
D
E
F
G
H
I
J
K
L
M
N
O
P
Q
R
S
T
U
V
W
X
Y
Z

A A

A
B
C
D
E
F
G
H
I
J
K
L
M
N
O
P
Q
R
S
T
U
V
W
X
Y
Z

A A

A
B
C
D
E
F
G
H
I
J
K
L
M
N
O
P
Q
R
S
T
U
V
W
X
Y
Z

A OA

A
B
C
D
E
F
G
H
I
J
K
L
M
N
O
P
Q
R
S
T
U
V
W
X
Y
Z

A O

A
B
C
D
E
F
G
H
I
J
K
L
M
N
O
P
Q
R
S
T
U
V
W
X
Y
Z

633 erences therein. The aerosol optical properties in OsloCTM3 are described in Myhre et
 634 al. (2007) with some recent updates, where the BC mass absorption coefficient (MAC)
 635 is following the formula in Zanatta et al. (2016) and a weak absorption implemented for
 636 OA (Lund et al., 2018).

637 Appendix B

638 Figure B1 shows the regional AOD biases of the AeroCom models relative to MISR
 639 retrievals (left panels) and the regional SW flux biases due to AOD biases (relative to
 640 MISR retrievals) and land surface albedo biases (relative to MODIS retrievals) calcu-
 641 lated from their radiative kernels (right panels) for April 2010. Many of the regional AOD
 642 bias patterns shown here are very similar to the AOD biases shown in Figure 9. The SW
 643 flux biases calculated from the radiative kernels using MISR AODs also resemble those
 644 shown in Figure 8. However, the biases over the tropical oceans are much muted when
 645 MISR AOD is used. The correlation coefficients between F and $F_{AOD} + F$ range
 646 from 0.79 to 0.94 over land, which is very similar to those derived when MODIS AOD
 647 is used. The correlation coefficients between F and F_{AOD} range from 0.26 to 0.63
 648 over ocean, not as high as when MODIS AOD is used. The reduced correlation over ocean
 649 is partly due to retrieval differences between MODIS and MISR, but largely due to MISR
 650 sampling issue as evident in the stripping features of the AOD bias plots.

651 Acknowledgments

652 All AeroCom simulations are available at the Norwegian Meteorological Institute. The
 653 CERES EBAF Ed4.1 data were obtained from <https://ceres.larc.nasa.gov/data/>. MODIS
 654 495 MYD08_M3_0_6_1 550 nm AOD Dark Target+Deep Blue Combined data were ob-
 655 tained from the Giovanni online data system, developed and maintained by the NASA
 656 GES DISC. The V6 MODIS Bidirectional Reflectance Distribution Function (BRDF)/albedo
 657 products (MCD43C1) were obtained from the Land Processes Distributed Active Archive
 658 Center (LP DACC) through <https://lpdaac.usgs.gov/products/mcd43c1v006/>.

659 This research has been supported by NASA CERES project. We would like to thank
 660 Dr. John P. Dunne for providing constructive comments on an earlier version of the pa-
 661 per. Ragnhild B. Skeie and Gunnar Myhre were funded through the Norwegian Research
 662 Council (grant no. 250573) and the European Union's Horizon 2020 Research and In-
 663 novation Programme under Grant Agreement 820829 (CONSTRAIN). Hitoshi Matsui
 664 was supported by the Ministry of Education, Culture, Sports, Science and Technology
 665 of Japan and the Japan Society for the Promotion of Science (MEXT/JSPS) KAKENHI
 666 Grant Numbers JP17H04709, JP16H01770, JP19H04253, JP19H05699, JP19KK0265,
 667 JP20H00196, and JP20H00638, MEXT Arctic Challenge for Sustainability (ArCS, JP-
 668 MXD1300000000) and ArCS-II (JPMDX1420318865) projects, and the Environment Re-
 669 search and Technology Development Fund 2-2003 (JPMEERF20202003) of the Environ-
 670 mental Restoration and Conservation Agency. David Neubauer acknowledges funding
 671 from the European Union's Horizon 2020 Research and Innovation programme, project
 672 FORCeS, under grant agreement no. 821205. The ECHAM-HAMMOZ model is devel-
 673 oped by a consortium composed of ETH Zurich, Max-Planck-Institut für Meteorologie,
 674 Forschungszentrum Jülich, University of Oxford, the Finnish Meteorological Institute,
 675 and the Leibniz Institute for Tropospheric Research and managed by the Center for Cli-
 676 mate Systems Modeling (C2SM) at ETH Zurich. Toshihiko Takemura is supported by
 677 the Japan Society for the Promotion of Science (JSPS) KAKENHI (grant no. JP19H05669),
 678 the Environment Research and Technology Development Fund (S-20) of the Environ-
 679 mental Restoration and Conservation Agency, Japan, and the NEC SX supercomputer
 680 system of the National Institute for Environmental Studies, Japan. Susanne E. Bauer
 681 and Kostas Tsigaridis acknowledge funding from the NASA Modeling, Analysis and Pre-
 682 diction Program. Resources supporting this work were provided by the NASA High?End

Figure B1.

- HOCH**
E., 3, 593628. d105194135932020
- AMBROSIO**
F. (2019) **High-resolution climate projections for the Amazon basin**. *Environ Monit Assess*, 14431475. d1051941214432019
- AMBROSIO**
F. (2001) **Spatial patterns of rainfall variability in the Amazon basin**. *J. Hydrol.*, 248, 2025520273.
- AMBROSIO**
F. (2021) **Climate change projections for the Amazon basin**. *Environ Monit Assess*, 1872021. d10519413692018
- AMMEND**
T. L. (2018) **Modeling the impact of deforestation on the Amazon rainforest**. *Environ Monit Assess*, 10519413692018. d10519413692018
- AMMEND**
G. (2001) **Amazonian hydrology**. *J. Hydrol.*, 248, 1206712097.
- AMMEND**
G. (2008) **Amazonian hydrology**. *Environ Monit Assess*, 1010292008009944. d1010292004021180
- AMMEND** (2004) **Amazonian hydrology**. *Environ Monit Assess*, 1010381043. d1010381043
- AMMEND**
L. (1996) **Amazonian hydrology**. *Environ Monit Assess*, 7, 437472.
- AMMEND** (2006) **Amazonian hydrology**. *Environ Monit Assess*, 6, 18151834.
- AMMEND**
L. (2013) **Amazonian hydrology**. *Environ Monit Assess*, 6, 29893034. d105194129892013
- AMMEND** (1992) **Amazonian hydrology**. *Environ Monit Assess*, 1, 276292.
- AMMEND** (2018) **Amazonian hydrology**. *Environ Monit Assess*, 895918. d1011751702081
- AMMEND** (2005) **Amazonian hydrology**. *Environ Monit Assess*, 35063526.
- AMMEND** (2016) **Amazonian hydrology**. *Environ Monit Assess*, 8182. d10519413692018

- 1033908030182
ENOMI 2021) **6**
2002. **JR**,
B (2020) **DB4090**) **d1010292020DB4090**
- ENOMI**.
W2020) M
DB4090
B, 4 (5) **d1010292019DB6705**
- ENOMI**
S.. W 2009) **DB4090**
B **JR**, 2, 748766. **d101175**
2008DB6371
- ENOMI** 2000) **M**
DB4090
B, 8, 977998.
- ENOMI**
... **W2018) DB4090**
DB1750 to 2014 **DB4090**
B **JR**, 1 (2) **d1010294931. d**
105194DB14909201
- ENOMI**
W2003) DB4090
B **JR**, 8, . **d1010292002DB2263**
- ENOMI** 2017) **DB4090**
B **JR**, **JAS**, 9, 19211947.
- ENOMI** 2018) **DB4090**
B **JR**, 98446) **d10103841467018056354**
- ENOMI** 2017) **DB4090**
B **JR**, **JAS**, 9, 18871920. **d101022017DB00937**
- ENOMI** 2020) **DB4090**
B **JR**, 4 (2020) **DB8978**) **d1010292020DB8978**
- ENOMI** 2019) **DB4090** 12 (1)
B **JR**, 1 (4) **d1010292018DB1400**
- ENOMI** 2006) **DB4090**
B **JR**, 1 (6) **d1010292005DB5796**
- ENOMI** 1986)
B **JR**, 1010079783459400946682 _16
- ENOMI** 2020) **DB4090**
B **JR**, 2 (8) **d1010292019DB1824**
- ENOMI**
D2007) DB4090
B **JR**, 9 (1) **d1011116000889200600226x**
- ENOMI**

- ...
.. bC 2013) **Witten**
...
1051941318532013
DG 2011) **Gill**
...
B, 1, 86358659. d105194186352011
HORN HW 2018) **C**
...
10519418132652018
HORN HEP
2008) **Gill**
...
1010292007D09334
HRB 2013) **Röhl**
...
20027
KASPERL JP
2013) **Hansh**
...
B, 3, 623472379. d1051941323472013
HAU J 2006) **Witt**
...
B, 6, 237253.
ROCKHAG
2013) **Witt**
...
d101109D0132243457
HARMSBT
2009) **Dittric**
...
d1010292008D10669
SANMIGUEL
M 2014) **RE** **Witt**
...
B, 9, 1396513989. d1010022014D22453
KOBAYASHI R
D 2002) **SP**
...
101016D03442570200913
EVANS 2009) **Witt**
...
B, 7(2014). d1010881755130771012014
HRB 2006) **R**
...
B, 6, 52255246.
ROCKHAG S
P 2020) **Witt**
...
12457. d10519410124312020
EVAN 2008) **Witt**
...
B, 9, 27792793. d101016D00807013
CONNISTEN

- ... H (2012) **H**
H, 56(1441)1469. doi:10.1941/14412012
- S**
S (2013) **H**
H
H, 3(6)32453270. doi:10.1941/332452013
- S** (2010) **H**
H
H
H, 5(1105)1105. doi:10.1029/2009JD12490
- S** (2013) **H**
H
H
H, 8, 145. doi:10.1029/2012JD18294
- H**
H (2010) **H**
H, 5(101)101. doi:10.1029/2009JD12665
- H**
H (2009) **A**
H
H, 30613073. doi:10.1941/30612009
- H** (2005) **H**
H
H, 101029200405029
- H** (2019) **H**
H
H, 2(7)27272765. doi:10.1941/227272019
- H**
N. H. (2019) **H**
H, 2, 16431677. doi:10.1941/216432019
- H** (2020) **H**
H
H, 606691
- H** (2013) **H**
H
H, 8(1)220235. doi:10.1029/2012JD18165
- H** (2013) **H**
H
H
H, 101029201208619
- H**
H (2016) **H**
H
R, 2, 59485971. doi:10.1002/2015JD24326
- H** (2021) **H**
H
H
H, 10103841612020001592
- H**
H (2012) **H**
H

- Sens. Environ., 117, 264-280. doi: 10.1016/j.rse.2011.10.002

Wang, Z., Schaaf, C. B., Strahler, A. H., Chopping, M. J., Roman, M. O., Shuai, Y., ... Fitzjarrald, D. R. (2014). Evaluation of MODIS albedo product (MCD43A) over grassland, agriculture and forest surface types during dormant and snow-covered period. Remote Sens. Environ., 140, 60-77. doi: 10.1016/j.rse.2013.08.025

Wielicki, B. A., Barkstrom, B. R., Harrison, E. F., Lee, R. B., Smith, G. L., & Cooper, J. E. (1996). Clouds and the Earth's Radiant Energy System (CERES): An Earth Observing System experiment. Bull. Amer. Meteor. Soc., 77, 853-868.

Wild, M., Folini, D., Schar, C., Loeb, N. G., Dutton, E. G., & Konig-Langlo, G. (2013). The global energy balance from a surface perspective. Clim. Dyn., 40, 3107-3134. doi: 10.1007/s00382-012-1569-8

Yu, H., Kaufman, Y. J., Chin, M., Feingold, G., Remer, L. A., Anderson, T. L., & coauthors. (2006). A review of measurement-based assessments of the aerosol direct radiative effect and forcing. Atmos. Chem. Phys., 6, 613-666.

Zanatta, M., Gysel, M., Bukowiecki, T., N. and Müller, Weingartner, E., Areskoug, H., Fiebig, M., ... Laj, P. (2016). A European aerosol phenomenology-5: Climatology of black carbon optical properties at 9 regional background sites across Europe. Atmos. Environ., 145, 1352-2310. doi: 10.1016/j.atmosenv.2016.09.035

Zhao, M., Golaz, J.-C., Held, I. M., Guo, H., Balaji, V., Benson, R., ... Xiang, B. (2018). The GFDL Global Atmosphere and Land Model AM4.0/LM4.0: 1. Simulation Characteristics With Prescribed SSTs. Journal of Advances in Modeling Earth Systems 10(3), 691-734. doi: 10.1002/2017MS001208